Carbohydrate Polymers 87 (2012) 901–909

Contents lists available at SciVerse ScienceDirect

Carbohydrate Polymers

journal homepage: www.elsevier.com/locate/carbpol

Preparation and characterization of TiO_2-regenerated cellulose inorganic–polymer hybrid membranes for dehydration of caprolactam

Tianrong Zhu [a], Yanwen Lin [a], Yunbai Luo [a], Xuan Hu [b], Wenhai Lin [a,b], Ping Yu [a,*], Chi Huang [a,*]

[a] Department of Applied Chemistry, College of Chemistry and Molecular Sciences, Wuhan University, Wuhan 430072, PR China
[b] Department of Environmental Science, College of Forestry, Central South University of Forestry and Technology, Changsha 410004, PR China

ARTICLE INFO

Article history:
Received 19 July 2011
Received in revised form 25 August 2011
Accepted 28 August 2011
Available online 3 September 2011

Keywords:
Regenerated cellulose
Nano-TiO_2
Inorganic–polymer hybrid membrane
Pervaporation
Caprolactam–water solutions

ABSTRACT

Novel membrane of inorganic–polymer hybrid membrane was prepared by incorporation of the nano-TiO_2 into regenerated cellulose (RC). The resulting membrane was characterized by AFM, SEM, and XRD. TiO_2 particles formed on the surface and in the interior of the hybrid membrane due to the TiO_2 conglomeration, and the surface roughness of the hybrid membrane increased linearly with increasing TiO_2 content. The membrane was tested for their ability to separate caprolactam–water mixtures by pervaporation. Among all the prepared membranes, RC-TiO_2 inorganic–polymer hybrid membrane containing 5 wt.% TiO_2 exhibited the good pervaporation performance with a flux of 1787.3 g m^{-2} h^{-1} and separation factor of 55091.7 at 328 K for 50 wt.% caprolactam. Besides, the normalized permeation fluxes in terms of water permeance, caprolactam permeance and selectivity were also introduced to evaluate the membranes performance. The activation energies were calculated using Arrhenius equation.

1. Introduction

Cellulose, obtained from wood pulp and cotton, is considered as being the richest and useful renewable material. Regenerated cellulose (RC) membranes were prepared from cotton, which have been widely applied to membrane separation techniques such as dialysis, ultrafiltration and purification of mixtures, due to hydrophilicity, solute permeability and solvent resistant (Chang, Zhang, Zhou, Zhang, & Kennedy, 2010; Ruan, Zhang, Mao, & Zeng, 2004). The RC membrane exhibits a high hydrophilicity, so it is a good candidate for pervaporation (Nagy, Borla, & Ujhidy, 1980). This membrane with higher permeation flux was used in pervaporation for separation ethanol–water mixtures (Yang, Zhang, Peng, & Zhong, 2000).

Pervaporation (PV) has attracted considerable attention currently because it can be operated at lower temperatures than other separation methods. Over several decades, PV was mainly focused on separation of aqueous–organic azeotropes, closely boiling mixtures, isomers, and now it has emerged as a good choice for separating heat sensitive products (Anjali Devi, Smitha, Sridhar, & Aminabhavi, 2006; Nunes & Peinemann, 2001). Caprolactam ($C_6H_{11}NO$) is a very heat-sensitive substance, which is synthesized via the cyclohexanone oximation and Beckmann rearrangement route using highly concentrated sulfuric acid and neutralizing the reaction mixture with aqueous ammonia (Mao & Wu, 2007). Water is the most important impurity in the final caprolactam purification because the existence of water can hinder the growth of molecular weight (Ragaini, Guaita, & Pirola, 2007). To prevent decomposition, various separation processes (i.e. thin-film distillation, crystallization under reduced pressure, distillation through triple-effect evaporation sets and melt crystallization by suspension) are usually employed for dehydration of caprolactam (Poschmann & Ulrich, 1996). But these processes suffer from high operating costs and high energy consumption. Moreover, the pollutants are transferred from one phase to another. Therefore, it is necessary to develop a new dehydration process for the concentrate of caprolactam–water mixtures. The application of PV as a means to achieve dehydration of caprolactam has been studied by Zhang, Yu, and Luo (2007a), who tried to remove the water from caprolactam–water mixtures through a poly(vinyl alcohol) membrane crosslinked with glutaraldehyde. A good permeation flux was obtained though the separation factor was not very good.

As for caprolactam–water mixtures, water is more hydrophilic and polar than caprolactam due to dipole moment of hydroxyl group. Furthermore, the molecular size of water is smaller than caprolactam. So water is both preferentially sorped and transported in the hydrophilic membranes. Accordingly, the molecular size and polarity difference should be a key factor to obtain a higher permselectivity (Chen, Liu, & Fang, 2007). So the RC membrane is a good choice for PV dehydration of caprolactam. However, the wide application of RC membrane is limited by lack

* Corresponding authors. Tel.: +86 27 68752511; fax: +86 27 68752511.
E-mail addresses: yuping@whu.edu.cn (P. Yu), chihuang@whu.edu.cn (C. Huang).

0144-8617/$ – see front matter © 2011 Elsevier Ltd. All rights reserved.
doi:10.1016/j.carbpol.2011.08.088

Nomenclature

J_i [g m^{-2} h^{-1}] permeation flux of component i
J [g m^{-2} h^{-1}] pervapor2ation permeation flux
D_i [m^2/s] diffusion coefficient of component i
S_i [mol/(m^3 Pa)] adsorption coefficient of component i
δ [m] membrane thickness
$p_{i,\text{feed}}$ [kPa] vapor pressure of component i in feed
$p_{i,\text{permeate}}$ [kPa] vapor pressure of component i in permeate
P_i [g/(m^2 h kPa)] membrane permeance component i
x_i [–] mole fraction of component i in the feed
y_i [–] mole fraction of component i in the permeate
$p^0_{i,\text{feed}}$[kPa] saturation vapor pressure of pure i in the feed liquid temperature
p_{permeate} [kPa] permeate pressure
J_0 [g m^{-2} h^{-1}] pre-exponential factor of the permeation flux from the Arrhenius equation
E_J [kJ/mol] apparent activation energy of the flux (kJ/mol)
E_P [kJ/mol] apparent activation energy of the permeance (kJ/mol)
E_D [kJ/mol] activation energy of the diffusion (kJ/mol)
R [J mol^{-1} K^{-1}] gas constant
T [K] absolute temperature
A [m^2] effective membrane area
W [g] weight of penetrant
t [h] permeation measuring time

Greek letters
β_{membrane} [–] membrane selectivity
α [–] pervaporation selectivity
γ_i [–] activity coefficient of component i in the feed

Subscript
i [–] component i, either water or caprolactam
1 [–] water
2 [–] caprolactam

of good separation factor. Inorganic–polymer hybrid membranes have attracted considerable attention as potential "next generation" membrane materials (Adoor, Sairam, Manjeshwar, Raju, & Aminabhavi, 2006; Bhat, Mallikarjuna, & Aminabhavi, 2006a; Bhat et al., 2006b; Bhat & Aminabhavi, 2006c; Naidu & Aminabhavi, 2005; Patil, Veerapur, Patil, Madhusoodana, & Aminabhavi, 2007; Sairam, Naidu, Nataraj, Sreedhar, & Aminabhavi, 2006a), because they have the synergistic to combine the desired properties of organic and inorganic systems (Chen, Liu, & Zhu, 2008). Recently, the inorganic materials including SiO_2 (Razavi, Sabetghadam, & Mohammadi, 2011), carbon nanotube (Liu, Chen, & Chang, 2009; Shirazi, Tofighy, & Mohammadi, 2011), $H_{14}[NaP_5W_{30}O_{110}]$ (Magalad, Gokavi, Nadagouda, & Aminabhavi, 2011), Al-MCM-41 (Magalad, Supale, Maradur, Gokavi, & Aminabhavi, 2010a), TiO_2 (Aminabhavi & Patil, 2010; Reddy et al., 2007; Sairam, Patil, Veerapur, Patil, & Aminabhavi, 2006b) were incorporated into polymer. Nano-TiO_2 as an active nano-material has many advantages such as innocuity, resisting and decomposing bacterias, UV resistance and super hydrophilicity (Yang, Zhang, Wang, Zheng, & Li, 2007). Moreover, TiO_2 can also be used in harsh conditions for its high chemical and thermal stability. The nanoparticles can create preferential permeation pathways for selective permeation while posing a barrier for undesired permeation in order to improve separation performance (Jadav & Singh, 2009).

In this paper, novel inorganic–polymer hybrid membranes via hybridization of cellulose with nano-TiO_2 were prepared by the phase inversion method. The aim of this work was to improve the performance of RC membrane effectively with the addition of nano-TiO_2 particles. Nano-TiO_2 particles dispersed in the membrane will favor the diffusion of penetrant. The effect of nano-TiO_2 content on the swelling and PV characteristics was studied. Particularly, the normalized permeation fluxes in terms of water permeance, caprolactam permeance and selectivity were calculated to evaluate the membranes performance.

2. Experimental

2.1. Material

The cellulose (cotton linter pulp) was provided by Hubei Chemical Fiber Group Ltd. (Xiangfan, China), and the α-cellulose content was more than 95%. The cellulose was used without further purification and its viscosity–average molecular weight (M) was determined to be 10.1×10^4. The pulp sheets of cellulose were shredded and dried for 8 h in a vacuum oven, stored in a desiccator until used. Nano-titanium dioxide (TiO_2, around 21 nm) was purchased from Germany. Caprolactam (chemical pure) was obtained from Baling Petrochemical Co. Ltd (SINOPEC, China). All the chemicals were used without further purification. Deionized water was used in preparing the aqueous feed solutions for the pervaporation experiments.

2.2. Preparation of nano-TiO_2 filled regenerated cellulose membranes

The TiO_2–cellulose hybrid membranes were prepared by the phase inversion method. Firstly, for preparing cellulose solution, 0.6 g of cotton linter and different concentrations (0, 1, 3, 5, and 7 wt.%) of TiO_2 nanopowder were added in 19.4 g of 7 wt.% NaOH/12 wt.% urea aqueous solvents and stirred for 5 min to obtain a slurry according to Cai et al. (2004). The polymer slurry was stored in a refrigerator (−10 °C) for about 24 h. The frozen solid was then melted at room temperature along with full stirring to obtain a uniform casting suspension. The suspensions were cast uniformly onto a glass plate by means of a hand-casting knife and then were immediately immersed in a 5 wt.% H_2SO_4 aqueous bath (15 °C). The nonporous structure of RC membrane is optically observed (see Fig. 1) when the temperature of coagulation bath is lower than 20 °C, owing to that the low temperature of coagulant interferes the coagulation rate. After complete coagulation, the regenerated cellulose (RC) membranes were peeled off and subsequently washed thoroughly with deionized water to remove residual solvent until neutrality. Finally, the membranes dried in air on a clean Plexiglas with the thickness of 40 μm. The RC-TiO_2 membranes according to the different concentrations (0, 1, 3, 5, and 7 wt.%) of TiO_2 nanopowder in membranes were designated as RC-0 to 7, respectively.

2.3. Particle size measurement of TiO_2

The size distributions of TiO_2 were recorded by means of dynamic light scattering method on a ZetaSizer (Model Nano ZS, Malvern, UK). TiO_2 particles were dispersed in water. After sonicating for 1 h, the solution was taken in a cuvette subjected to laser beam radiation. The equipment can measure particles from 0.6 nm to 6 μm with a detector at position 173° to measure the intensity of the scattered light.

2.4. Characterization of membranes

2.4.1. Atomic force microscope (AFM)

The surface roughness of the membranes was determined by AFM analysis (SPM-9500J3, SHIMADZU, Kyoto, Japan), quantified by root mean square (RMS) roughness. RMS was determined over

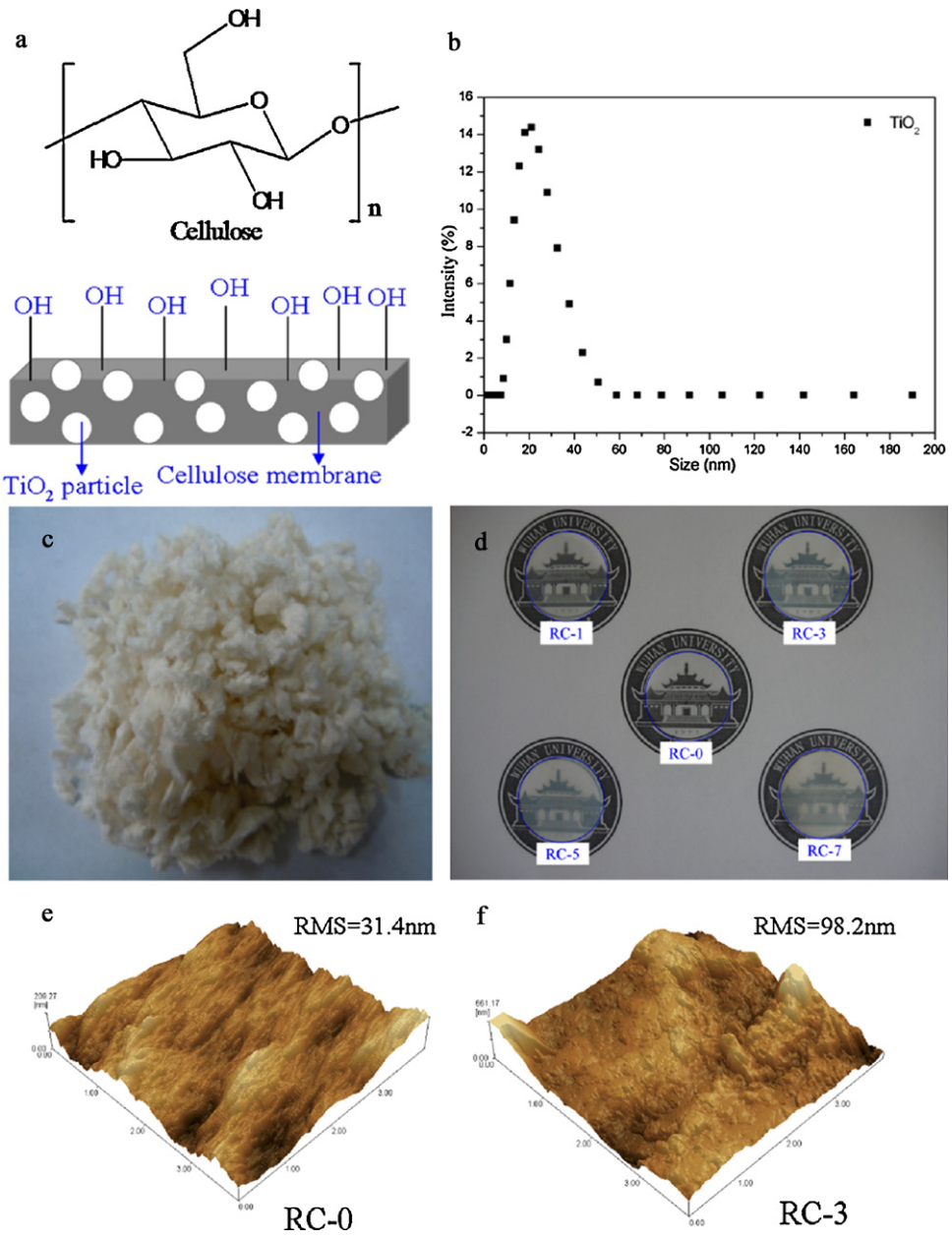

Fig. 1. Molecular structure of cellulose, the size distribution of dispersion TiO_2 and photographs of cotton and TiO_2 filled cellulose membrane. (a) Cellulose, (b) TiO_2, (c) cotton, (b and d) TiO_2 filled cellulose membrane, (e and f) 3D AFM images of RC-0 and RC-3 membranes.

an area of 4 μm × 4 μm. All the roughness parameters were calculated by the software.

2.4.2. Scanning electron microscopy (SEM)

SEM was used to study the morphology of the hybrid membranes. All specimens were coated with a conductive layer of sputtered gold. The morphologies of nano-TiO_2 filled RC membranes were observed with SEM (FEI Quanta 200, Holland).

2.4.3. X-ray diffraction (XRD)

The XRD patterns of the membrane samples were characterized by a Germany Bruker D8 Advance X-ray diffractometer using Cu Kα radiation. The angle of diffraction was varied from 8° to 40° using a step size of 0.02°.

2.5. Swelling experiments

The dry TiO_2–RC hybrid membranes were weighed before being immersed in feed mixtures of caprolactam–water at 40 °C in a thermostatic bath. The swollen membrane sample was taken out from the solution, wiped with filter paper to remove the surface liquid, and then quickly weighed. The membranes were placed on a single-pan electronic balance (model EL204, METTLER Toledo) sensitive to ±0.1 mg. All experiments were repeated at least three times. The results were averaged.

The degree of swelling (DS) was calculated by

$$\mathrm{DS} = \frac{(W_s - W_d)}{W_d} \quad (1)$$

where W_d and W_s were the weights of the dried and swollen membranes, respectively.

2.6. Pervaporation experiments

The experimental pervaporation set–up was used as reported in our previous article (Zhu, Luo, Lin, Li, & Yu, 2010). The membrane was installed in a stainless-steel membrane cell with the effective surface area of 51.53 cm^2 in contact with the feed mixture. The feed solution was continuously circulated from a feed tank at a relatively high flow rate of 200 L/h to the upstream side of the membrane in the cell at the desired temperature by a pump. The feed temperature in the range of 40–60 °C was monitored by a digital vacuometer. Pervaporation experiments were carried out by maintaining atmospheric pressure on the feed side while on the permeate side about 10 mbar within ±1 mbar with a vacuum pump. Upon reaching steady-state conditions which was obtained after about 1 h throughout the experiments, permeate vapor was collected in liquid nitrogen traps with certain intervals, and weighted to calculate the permeate flux. The composition of permeate was determined by GC to calculate the separation factor. Here the composition of the condensed liquid was analyzed by a SP3400 gas chromatography with a FID detector (made in China) under the following conditions: PEG-20 M capillary column, 2 m × 6 mm i.d.; temperature, 170 °C; carrier gas, nitrogen; flow rate, 30 mL min^{-1} (Zhang et al., 2007a). The compositions of the liquid feed mixtures were analyzed by measuring the refractive index within an accuracy of ±0.0001 units using high-precision Abbe Refractometer (Atago NAR-3T, Japan), which can be calculated by using previously established standard graph of refractive index versus known mixture composition ($y_{caprolactamn} = 0.1704_{water} + 1.3303$, $R^2 = 0.9999$). The refractometer prism was maintained at 25 ± 0.1 °C.

The permeation flux (J, g m^{-2} h^{-1}) was defined as follows:

$$J(\text{g m}^{-2}\,\text{h}^{-1}) = \frac{W}{(A \times t)} \tag{2}$$

where W(g) is the weight of penetrant, A(m^2) is the effective membrane area and t(h) is the measuring time.

The separation factor α was calculated by:

$$\alpha = \left(\frac{y_{water}/y_{caprolctam}}{x_{water}/x_{caprolctam}} \right) \tag{3}$$

where $x_{water}, x_{caprolactam}$ and $y_{water}, y_{caprolactam}$ are the mole fraction of water and caprolactam in the feed and permeate, respectively.

In order to distinguish between the intrinsic membrane properties and the influence of the experimental operation conditions, normalized permeation flux (permeance) and membrane selectivity were proposed and evaluated to clarify the contribution by the nature of the membrane to separation performance. The driving force in pervaporation is a gradient in chemical potential across the membrane, which can be expressed in experimentally measurable quantities such as partial pressures. The permeate side is considered to be negligible if the downstream pressures applied are close to vacuum. The basic transport equation for pervaporation can be written as (Wijmans, 2003):

$$J_i = \frac{(D_i S_i)}{\delta(p_{i,\text{feed}} - p_{i,\text{permeate}})} = P_i(p_{i,\text{feed}} - p_{i,\text{permeate}}) \tag{4}$$

On the basis of Raoult's law (feed side) and Dalton's law (permeate side) it is equal:

$$J_i = P_i(x_i \gamma_i p^o_{i,\text{feed}} - y_i p_{\text{permeate}}) \tag{5}$$

where J_i is the permeation flux, P_i is the permeance of the membrane for i (which equals the permeability coefficient divided by the membrane thickness), x_i, y_i are the mole fraction of i in the feed and the permeate, respectively, γ_i is the activity coefficient of i in the feed liquid and $p^o_{i,\text{feed}}$ is the saturation vapor pressure of pure i in the feed liquid temperature, p_{permeate} is the permeate pressure.

The activity coefficient of water (γ_1) and caprolactam (γ_2) can be calculated by using Van Laar equation:

$$\text{Ln}\ (\gamma_i) = \frac{[A_1 A_2 x_2 x_1/(A_1 x_1 + A_2 x_2)]^2}{(x_i^2 \times A_i)}, \quad (i = 1, 2) \tag{6}$$

where $A_1 = -1.5810$ and $A_2 = -1.0429$. The $p^0_{i,\text{feed}}$ is determined from the Antoine equation:

$$\text{Log}\ (p^0_{i,\text{feed}}) = \frac{A_0 - B_0}{T + C_0} \tag{7}$$

where T is degree Celsius (°C). Coefficients for the Van Laar equation of $p^o_{1,\text{feed}}$ (water) used in the calculations: $A_0 = 8.07131$, $B_0 = 1730.630$ and $C_0 = 233.426$, while for $p^o_{2,\text{feed}}$ (caprolactam): $A_0 = 6.78000$, $B_0 = 2344.000$ and $C_0 = 273.150$.

The membrane selectivity (β_{mem}) is an intrinsic property of the membrane material, which is defined as the ratio of the water permeance over the caprolactam permeance.

$$\beta_{\text{membrane}} = \frac{P_{\text{water}}}{P_{\text{caprolactam}}} \tag{8}$$

3. Results and discussion

3.1. Membrane characterization

3.1.1. Photographs and 3D AFM analysis

Fig. 1(a–f) illustrates molecular structure of cellulose, the size distribution of dispersion TiO_2 and photographs of RC membrane by the incorporation of TiO_2. It can be seen from Fig. 1(b) that zeta average diameter of TiO_2 particles is around 21 nm. Fig. 1(d) shows that the optical transparency of hybrid membranes decreased gradually with increasing TiO_2 content. Fig. 1(e and f) shows the AFM images of the surface topography of the pure RC and its hybrid membranes with 3 wt.% of TiO_2. The surface of the pure RC membrane (Fig. 1(e)) is very regular because the polymer matrix shows minor undulations of the chains. While the polymer matrix surrounds the particle in the hybrid membrane (Fig. 1(f)) showing irregular surface topography (Al-Sagheer & Merchant, 2011). So the roughness of the hybrid membrane surface is higher than that of the RC-0 membrane because the TiO_2 dispersed on the surface and in the interior of the hybrid membranes due to the TiO_2 conglomeration. These rough surfaces will be in contact with the feed during pervaporation processes, which favors the feed diffusion (Zhang, Liu, Shi, & Xiong, 2008).

3.1.2. SEM analysis

Fig. 2 shows the SEM images of the top surface and cross-sectional views of the nano-TiO_2, pure RC and its nano-TiO_2 filled hybrid membranes. There are no flaws on the surface of the pure RC membrane. The nonporous structure of dense membrane is observed from the cross-section of the membrane. The thickness of membrane was found about 40 μm. It is clearly observed from Fig. 2(a) and (d–f) that the TiO_2 particles formed on the surface due to the TiO_2 conglomeration. The distribution of TiO_2 increased from membrane RC-3 to RC-7 with increasing the content of TiO_2. These findings indicate that the addition of TiO_2 nanoparticles has a large effect on membrane structure which might provide extra free volumes to the polymer chains, consequently to offer spaces for water molecules to permeate through the membranes.

3.1.3. XRD results

XRD curves of nano-TiO_2 powders, RC membrane and TiO_2–RC inorganic–polymer hybrid membranes are shown in Fig. 3. The pattern of TiO_2 crystal powders has two crystalline characteristic peaks at 2θ of 25.30° and 37.85° which agree with the literature

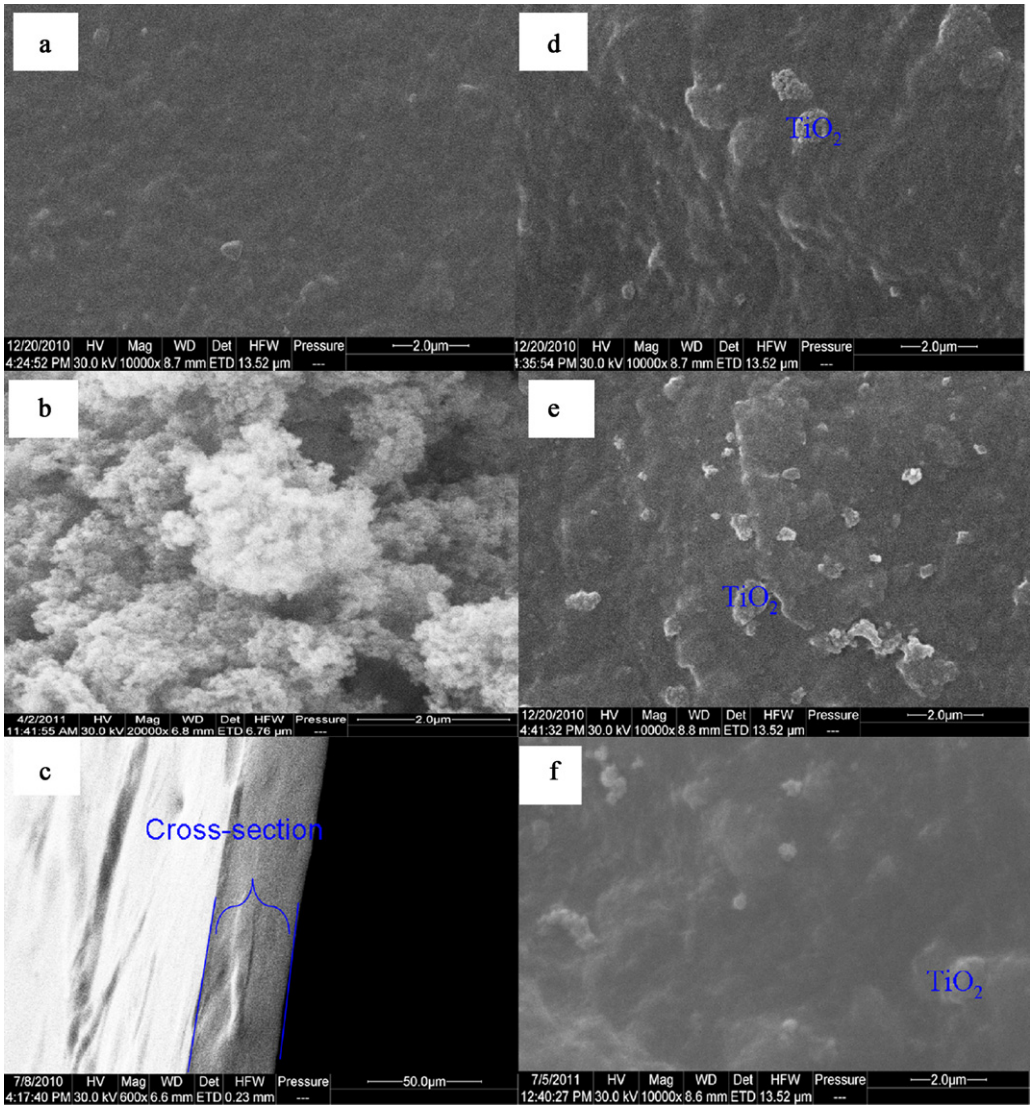

Fig. 2. Surface and cross-section SEM photographs of (a) RC-0, (b) TiO_2, (c and d) RC-3, (e) RC-5 and (f) RC-7 hybrid membranes.

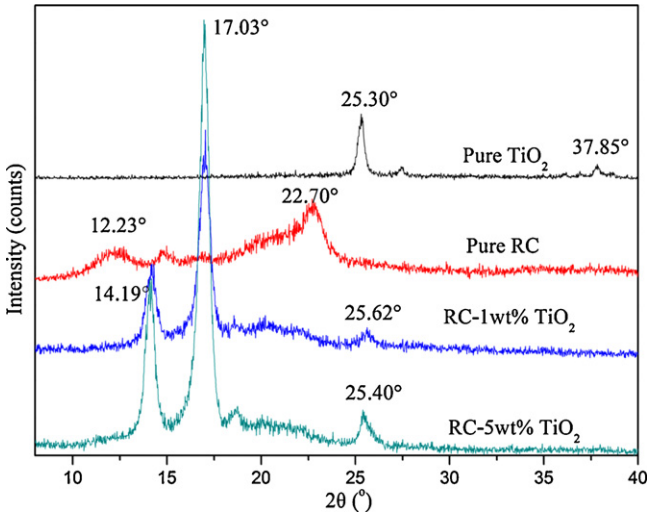

Fig. 3. XRD of pure RC membrane, RC-1 and RC-5 hybrid membranes.

report (Park et al., 1999). The pattern of TiO_2–RC hybrid membranes have a crystalline characteristic peak at $2\theta = 25.62^\circ$ that is analogous with the characteristic peak of TiO_2 crystal powders. However its location occurs slight shift, compared with the pattern of TiO_2 nanoparticles. But the location of the peaks at $2\theta = 37.85^\circ$ did not appear due to very small amount of TiO_2 present in RC matrix. It is clear that the peak intensity of the typical diffraction peak at 2θ of 14.19° and 17.03° due to the RC crystalline planes (Mao et al., 2010) increases with the introduction of the inorganic component.

3.2. Swelling characteristics

Fig. 4 displays swelling behavior of the hybrid membranes in different feed mixtures at 40 °C. Among all the membranes, RC-TiO_2 inorganic–polymer hybrid membrane containing 1 wt.% TiO_2 gave a slightly higher swelling. It is also observed that the addition of nano-TiO_2 particles into RC membranes attributed to a little lower swelling (Aminabhavi & Patil, 2010). When TiO_2 content was greater than 3 wt.%, a thicker skin layer was produced resulting in decrease the degree of swelling of the hybrid membranes. It

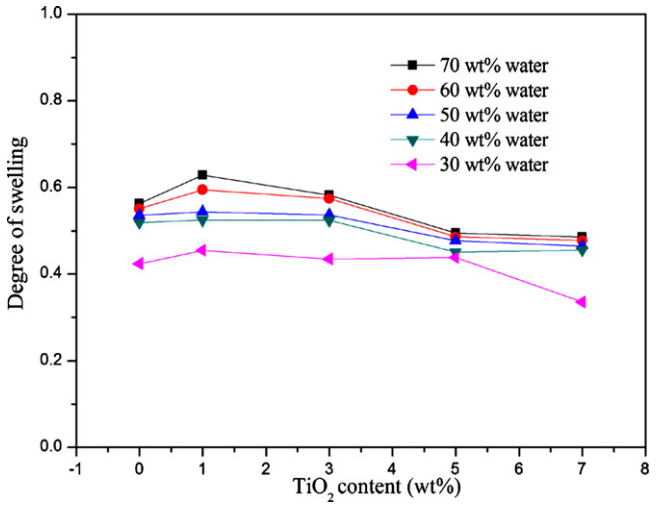

Fig. 4. Effect of TiO_2 content on the degree of swelling of RC-TiO_2 hybrid membranes for different caprolactam aqueous solutions.

also can be observed from the Fig. 4 that the degree of swelling increased with increasing water concentration. Since water has a better affinity towards the membranes than caprolactam.

3.3. PV performance results

3.3.1. Effect of TiO_2 content and feed concentration on PV performance

As shown in Fig. 5(a) and (c), the total flux and water permeance of the membrane increase initially and then decreases with the increase of TiO_2 content. It has a maximum flux and water permeance when TiO_2 content is 5 wt.%. The facts should be attributed to an increased selective interaction between water molecules and the membrane, since RC membranes contain –OH groups, which are capable of forming hydrogen bonds with the water molecules (Karidurаganavar, Varghese, Choudhari, & Olley, 2009). The facts should be attributed to an increased selective interaction between water molecules and the membrane, since RC membranes contain –OH groups which are capable of forming hydrogen bonds with the water molecules (Adoor, Manjeshwar, Bhat, & Aminabhavi, 2008; Patil & Aminabhavi, 2008; Veerapur, Patil, Gudasi, & Aminabhavi, 2008; Veerapur, Gudasi, & Aminabhavi, 2008). Moreover, the TiO_2 particle might provide preferential permeation pathways to the polymer chain increasing the permeabilities and diffusion coefficients. Consequently, the TiO_2 particles offer spaces for water and caprolactam molecules to permeate through the membranes. However high TiO_2 filler concentration (>5 wt.%) forms a thicker skin layer on the membrane surface (Yang et al., 2007), which slows down the sorption rate, resulting in a negative effect on the permeability.

The separation factor indicated by the water composition in permeate, increased with an increase in TiO_2 loading up 0 to 5 wt.% and then dropped when the TiO_2 content reached 7 wt.% (Fig. 5(b)). But the membrane selectivity (Fig. 5(d)) increases continuously with increasing amounts of TiO_2. The overall selectivity of a membrane is generally explained on the basis of interaction between membrane and the permeating molecules and the molecular size of the permeating species. The separation factor initially increased because the addition of TiO_2 creates some interfacial channels between the polymer chain and the TiO_2 exterior for selective permeation of water while posing a barrier for caprolactam. Another factor could be the intrinsic structure of membrane with the dense structure, which blocks the passage of caprolactam with a bulky group and collision diameter of 5.6 Å compared with water with a collision diameter of only 3.0 Å. However at higher concentration (>5 wt.%), the formation of large pores on the membrane surface caused by

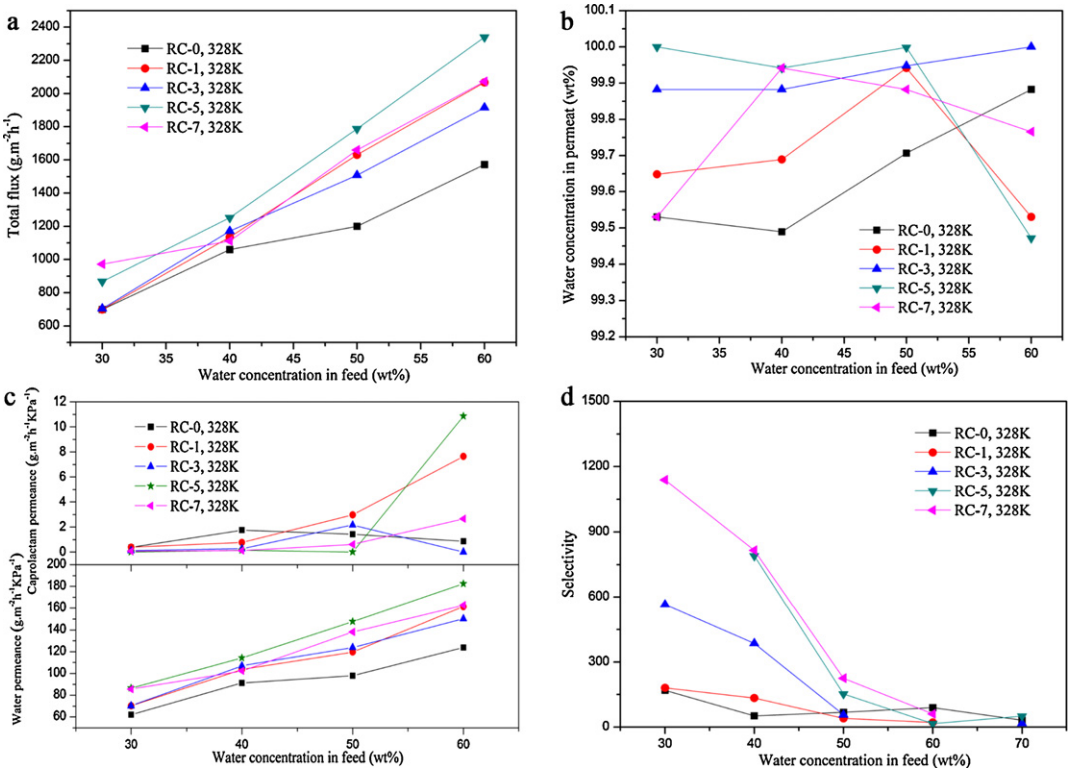

Fig. 5. Effect of TiO_2 content and the feed concentration on the pervaporation performances at different feed mixtures at 328 K: (a) total flux; (b) water concentration in permeate; (c) water and caprolactam permeance; (d) selectivity.

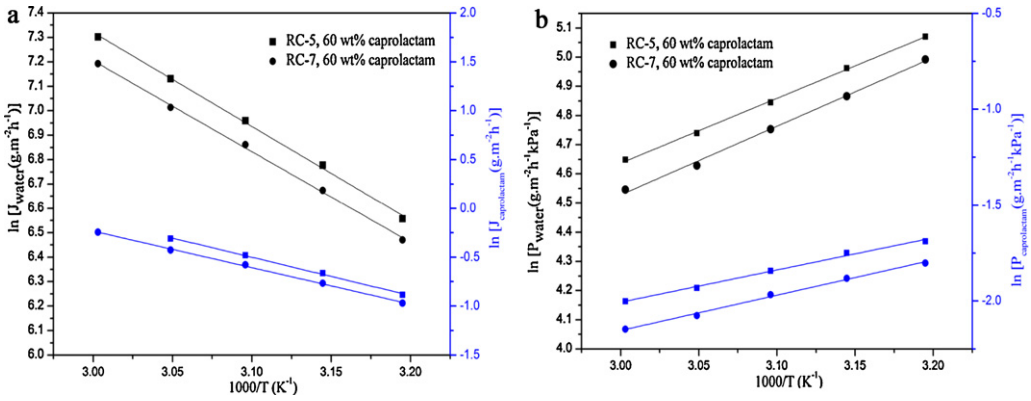

Fig. 6. Temperature dependence of (a) flux and (b) permeance for RC-5 and RC-7 at 60 wt.% caprolactam.

nanoparticles aggregate results in the decline of retention (Zhang et al., 2008). A promising result achieved for the TiO_2-incorporated RC membranes was that both the permeation flux and selectivity went up simultaneously with the increase of TiO_2 content in the range of 0–5 wt.%.

These figures indicate that not only the flux and permeance but also the separation factor and selectivity are strongly dependent on the feed composition. The feed concentration range from 30 to 70 wt.% of water was chosen by considering the concentration changes from the triple-effect evaporation sets. In addition, caprolactam aqueous solution becomes stiff and saturated when the caprolactam content in feed solution is above 70 wt.% at room temperature (Zhang et al., 2007a). It can be seen from Fig. 5(a) that with the water concentration from 30 to 70 wt.% the total flux increased. The higher fluxes can be explained by the strong interaction between water molecules and the membrane, since cellulose contains active groups which are capable of forming hydrogen bonds with the water molecules. As the water concentration in the feed increases, the amorphous regions of the membrane are more swollen and the polymer chains become more flexible. This results in both water and caprolactam molecules more easily penetrate through membranes. So the total flux was increased. But the separation factor indicated by the water composition in permeates (as shown in Fig. 5(b)) decreased. This trade-off was generally observed in pervaporation processes (Hyder, Huang, & Chen, 2009; Singha, Parya, & Ray, 2009). It also can be seen from Fig. 5(c) that the permeances of both water and caprolactam increase continuously with increasing water feed concentration. This implies the highly hydrophilic cellulose membrane material, resulting in the higher degree of swelling (Fig. 4). The sorption of the TiO_2–RC hybrid membrane increases with increasing amounts of water. It is interesting that caprolactam permeance also increases. This increase of caprolactam permeance with water feed concentration reveals a coupling effect between caprolactam and water permeation through the membrane. So the membrane selectivity values (Fig. 5(d)) decreased considerably, but are still higher than that observed for RC-0 (Magalad, Gokavi, Raju, & Aminabhavi, 2010b).

3.3.2. Activation energy

The temperature dependence of the pervaporation flux and permeance can be expressed by Arrhenius equations (Feng & Huang, 1996; Wang, Li, Lin, & Chen, 2009):

$$J_i = J_0 \exp\left(-\frac{E_J}{RT}\right) \tag{9}$$

$$P_i = P_0 \exp\left(-\frac{E_P}{RT}\right) \tag{10}$$

where J_0, P_0, E_J and E_P are the pre-exponential factor, apparent activation energy of the permeation flux and the membrane permeance, respectively. R indicates the gas constant ($J\,mol^{-1}\,K^{-1}$) and T is absolute temperature (K).

The difference between E_J and E_P is the molar heat of vaporization ΔH_V, expressed as follows.

$$\Delta H_V = E_J - E_P \tag{11}$$

Fig. 6 shows Arrhenius plots ($\ln J$ and $\ln P$ versus $1/T$) through TiO_2–RC hybrid membranes according to Eqs. (9) and (10). It can be found that the temperature dependence of the pervaporation permeance agrees well with the Arrhenius relationship. The evaluated values E_J, E_P and ΔH_V are presented in Table 1.

The negative value of activation energy of permeation E_P is observed from Table 1. This has been found to be the case for ethanol/water permeation through a polyion membrane, where the E_J values are 25.9 and 38.5 kJ/mol for water and ethanol, respectively, whereas their corresponding E_P values are −15.9 and −2.5 kJ/mol (Karakane, Tsuyumoto, Maeda, & Honda, 1991). E_P is the sum of the activation energy of diffusion E_D and the enthalpy of sorption ΔH. While E_D is generally positive, ΔH is usually negative for the exothermic sorption process. When the negative ΔH dominates over the positive E_D, negative value of E_P occurs, indicating that the membrane permeability coefficient decreases with increasing temperature (Feng & Huang, 1996).

As can be seen in Table 1, absolute value of E_P of both water and caprolactam is observed to be increasing, compared with the hybrid membrane of RC-5 with RC-7. These results suggest that the energy

Table 1
Activation energy data for RC-5 and RC-7 pervaporation membranes at 60 wt.% caprolactam.

Membrane	Activation energy (kJ/mol)					ΔH_V (kJ/mol)	
	E_P		E_J			Water	Caprolactam
	Water	Caprolactam	Water	Caprolactam	ΔE		
RC-5	−18.48	−13.98	31.97	32.55	0.58	50.45	46.53
RC-7	−19.59	−15.30	30.92	31.00	0.08	50.51	46.30

Table 2
Comparison of hybrid membrane separation performance with literatures.

Membranes	Thickness (±μm)	Caprolactam in feed (wt.%)	Temperature (°C)	Total flux ($g\,m^{-2}\,h^{-1}$)	Separation factor	Reference
PVA cross-linked with 0.5 wt.% Gal	25–35	50	50	900	575	Zhang, Yu, and Luo (2006)
PVA/PAN composite membranes	80–100	50	55	1802	890	Zhang et al. (2007a)
PVA/PES composite membranes	110 ± 5	50	55	790	200	Zhang, Yu, and Luo (2007b)
CS/PVA(1:3)/PAN composite membrane	100	50	50	757	443	Li, Yu, Zhu, and Zhang (2010)
GA cross-linked NaAlg–PVP composite membrane	80–100	50	50	1634.4	1610.6	Zhu et al. (2010)
RC-5 membrane	40	50	55	1787.3	55091.7	Present work

barrier for both water and caprolactam has increased. And then these two molecules can be more difficult to transport through the material. The penetrant permeance has become more temperature-dependence. The E_P of water of the RC-5 is lower than that of the RC-7, indicating that the water can be more readily transported through the RC-5 hybrid membrane.

Also in Table 1, the activation energies of water calculated from either the flux (E_J) or the permeance (E_P) are lower than those of caprolactam. Therefore, more energy is required for caprolactam molecules to transport across the membrane at the same conditions. The lower activation energies of water than caprolactam are reflected by the intrinsic properties of hydrophilic membrane materials. The positive value ΔE of ($E_{caprolactam}$ E_{water}) indicates that α decreases with an increase in temperature (Harogoppad & Aminabhavi, 1991).

As shown in Table 1, the molar heat of vaporization ΔH_V for water or caprolactam are almost the same between the two different blend membranes or caprolactam concentrations investigated, which is consistent with the previous reports in the dehydration of aqueous alcohol systems through filled-hydrophilic polymeric membranes (Huang, Guan, Tan, Qiao, & Kulprathipanja, 2006).

3.3.3. *Comparison of present membrane performance with the literature*

The total flux and selectivity from the present study (for 50 wt.% caprolactam at 50, 55 °C were compared with other inorganic–polymer hybrid membranes reported in literatures and presented in Table 2. Although the membranes are made from different material and preparation techniques, the dehydration performance of the nano-TiO_2 filled RC membrane prepared in this study shows a comparable, good flux and higher selectivity.

4. Conclusions

In this paper, TiO_2–cellulose inorganic–organic hybrid membranes were successfully prepared by phase-inversion method. The morphologies and properties of the resulting membrane were investigated using AFM, SEM and XRD characterization techniques. Adding TiO_2 to polymer casting solution greatly affected the morphologies and properties of the resulting membrane. Furthermore, these membranes were applied in caprolactam dehydration by pervaporation. The effects of nano-TiO_2 particles on pervaporation performances were investigated. The main conclusions are as follows:

(1) The structure of the RC membrane was changed by the incorporation of nano-TiO_2 particles. The AFM and SEM images revealed that the TiO_2 dispersed on the surface and in the interior of the RC membranes due to the TiO_2 conglomeration and the distribution of TiO_2 increased with increasing the content of TiO_2. With increasing TiO_2 nanoparticles concentration, XRD confirmed that crystallinity of membranes increased, which benefited to enhance the membrane selectivity.

(2) The performance of the RC membrane was improved by the addition of nano-TiO_2 particles. An increase of TiO_2 content in the membrane matrix results to a simultaneous increase of both permeation flux and selectivity. The TiO_2 particle might provide some interfacial channels between the polymer chain and the TiO_2 exterior leading to the enhanced permeabilities and diffusion rate, size discrimination and sorption capacity of water over caprolactam. The RC-5 exhibited the highest separation selectivity of 55091.7 with a flux of 1787.3 $g\,m^{-2}\,h^{-1}$ at 328 K for 50 wt.% of water in the feed.

(3) Negative value of E_P was obtained, indicating that the membrane permeability coefficient decreases with increasing temperature. The lower activation energies of water than caprolactam are reflected by the intrinsic properties of hydrophilic membrane materials.

Acknowledgements

This work was supported by the Plan of the National Sci-Tech Major Special Item for Water Pollution Control and Management (2009ZX07528-003-05) and the Fundamental Research Funds for the Central Universities (FRFCU), China (A ward no. 20102030201000043).

References

Adoor, S. G., Sairam, M., Manjeshwar, L. S., Raju, K. V. S. N., & Aminabhavi, T. M. (2006). Sodium montmorillonite clay loaded novel mixed matrix membranes of poly(vinyl alcohol) for pervaporation dehydration of aqueous mixtures of isopropanol and 1,4-dioxane. *Journal of Membrane Science*, *285*, 182–195.

Adoor, S. G., Manjeshwar, L. S., Bhat, S. D., & Aminabhavi, T. M. (2008). Aluminum-rich zeolite beta incorporated sodium alginate mixed matrix membranes for pervaporation dehydration and esterification of ethanol and acetic acid. *Journal of Membrane Science*, *318*, 233–246.

Al-Sagheer, F. A., & Merchant, S. (2011). Visco-elastic properties of chitosan-titania nano-composites. *Carbohydrate Polymers*, *85*, 356–362.

Aminabhavi, T. M., & Patil, M. B. (2010). Nanocomposite membranes of poly(vinyl alcohol) loaded with polyaniline-coated TiO_2 and TiO_2 nanoparticles for the pervaporation dehydration of aqueous mixtures of 1,4-dioxane and tetrahydrofuran. *Designed Monomers and Polymers*, *13*, 497–508.

Anjali Devi, D., Smitha, B., Sridhar, S., & Aminabhavi, T. M. (2006). Dehydration of 1,4-dioxane through blend membranes of poly(vinyl alcohol) and chitosan by pervaporation. *Journal of Membrane Science*, *280*, 138–147.

Bhat, S. D., Mallikarjuna, N. N., & Aminabhavi, T. M. (2006). Microporous aluminophosphate ($AlPO_4$-5) molecular sieve-loaded novel sodium alginate composite membranes for pervaporation dehydration of aqueous-organic mixtures near their azeotropic compositions. *Journal of Membrane Science*, *282*, 473–483.

Bhat, S. D., Naidu, B. V. K., Shanbhag, G. V., Halligudi, S. B., Sairam, M., & Aminabhavi, T. M. (2006). Mesoporous molecular sieve (MCM-41)-filled sodium alginate hybrid nanocomposite membranes for pervaporation separation of water–isopropanol mixtures. *Separation and Purification Technology*, *49*, 56–63.

Bhat, S. D., & Aminabhavi, T. M. (2006). Novel sodium alginate-Na+MMT hybrid composite membranes for pervaporation dehydration of isopropanol, 1,4-dioxane and tetrahydrofuran. *Separation and Purification Technology*, *51*, 85–94.

Cai, J., Zhang, L., Zhou, J., Li, H., Chen, H., & Jin, H. (2004). Novel fibers prepared from cellulose in NaOH/urea aqueous solution. *Macromolecular Rapid Communications*, *25*, 1558–1562.

Chang, C., Zhang, L., Zhou, J., Zhang, L., & Kennedy, J. F. (2010). Structure and properties of hydrogels prepared from cellulose in NaOH/urea aqueous solutions. *Carbohydrate Polymers*, *82*, 122–127.

Chen, J. H., Liu, Q. L., & Fang, J. (2007). Composite hybrid membrane of chitosan–silica in pervaporation separation of MeOH/DMC mixtures. *Journal of Colloid and Interface Science*, *316*, 580–588.

Chen, J. H., Liu, Q. L., & Zhu, A. M. (2008). Pervaporation separation of MeOH/DMC mixtures using STA/CS hybrid membranes. *Journal of Membrane Science*, *315*, 74–81.

Feng, X., & Huang, R. Y. M. (1996). Estimation of activation energy for permeation in pervaporation processes. *Journal of Membrane Science*, *118*, 127–131.

Harogoppad, S. B., & Aminabhavi, T. M. (1991). Diffusion and sorption of organic liquids through polymer membranes. 5. Neoprene, styrene–butadiene–rubber, ethylene–propylene–diene terpolymer, and natural rubber versus hydrocarbons (C_8–C_{16}). *Macromolecules*, *24*, 2598–2605.

Huang, Z., Guan, H. M., Tan, W. L., Qiao, X., & Kulprathipanja, S. (2006). Pervaporation study of aqueous ethanol solution through zeolite-incorporated multilayer poly(vinyl alcohol) membranes: Effect of zeolites. *Journal of Membrane Science*, *276*, 260–271.

Hyder, M. N., Huang, R. Y. M., & Chen, P. (2009). Composite poly(vinyl alcohol)-poly(sulfone) membranes crosslinked by trimesoyl chloride: characterization and dehydration of ethylene glycol–water mixtures. *Journal of Membrane Science*, *326*, 363–371.

Jadav, G. L., & Singh, P. S. (2009). Synthesis of novel silica-polyamide nanocomposite membrane with enhanced properties. *Journal of Membrane Science*, *328*, 257–267.

Karakane, H., Tsuyumoto, M., Maeda, Y., & Honda, Z. (1991). Separation of water–ethanol by pervaporation through polyion complex composite membrane. *Journal of Applied Polymer Science*, *42*, 3229–3239.

Kariduraganavar, M. Y., Varghese, J. G., Choudhari, S. K., & Olley, R. H. (2009). Organic–inorganic hybrid membranes: Solving the trade-off phenomenon between permeation flux and selectivity in pervaporation. *Industrial & Engineering Chemistry Research*, *48*, 4002–4013.

Li, Q., Yu, P., Zhu, T., & Zhang, L. (2010). Pervaporation performance of crosslinked PVA and chitosan membranes for dehydration of caprolactam solution. *Desalination and Water Treatment*, *16*, 304–312.

Liu, Y.-L, Chen, W.-H., & Chang, Y.-H. (2009). Preparation and properties of chitosan/carbon nanotube nanocomposites using poly(styrene sulfonic acid)-modified CNTs. *Carbohydrate Polymers*, *76*, 232–238.

Magalad, V. T., Gokavi, G. S., Nadagouda, M. N., & Aminabhavi, T. M. (2011). Pervaporation separation of water–ethanol mixtures using organic–inorganic nanocomposite membranes. *The Journal of Physical Chemistry C*, *115*, 14731–14744.

Magalad, V. T., Supale, A. R., Maradur, S. P., Gokavi, G. S., & Aminabhavi, T. M. (2010). Preyssler type heteropolyacid-incorporated highly water-selective sodium alginate-based inorganic–organic hybrid membranes for pervaporation dehydration of ethanol. *Chemical Engineering Journal*, *159*, 75–83.

Magalad, V. T., Gokavi, G. S., Raju, K. V. S. N., & Aminabhavi, T. M. (2010). Mixed matrix blend membranes of poly(vinyl alcohol)-poly(vinyl pyrrolidone) loaded with phosphomolybdic acid used in pervaporation dehydration of ethanol. *Journal of Membrane Science*, *354*, 150–161.

Mao, L., & Wu, B. (2007). A novel approach for one-step forming ε-caprolactam from cyclohexane nitrozation catalyzed by transition metal salt. *Chinese Chemical Letters*, *18*, 269–271.

Mao, Z., Cao, Y., Jie, X., Kang, G., Zhou, M., & Yuan, Q. (2010). Dehydration of isopropanol–water mixtures using a novel cellulose membrane prepared from cellulose/N-methylmorpholine-N-oxide/H_2O solution. *Separation and Purification Technology*, *72*, 28–33.

Nagy, E., Borla, U., & Ujhidy, A. (1980). Membrane permeation of water–alcohol binary mixtures. *Journal of Membrane Science*, *7*, 109–118.

Naidu, B. V. K., & Aminabhavi, T. M. (2005). Pervaporation separation of water/2-propanol mixtures by use of the blend membranes of sodium alginate and (hydroxyethyl)cellulose: roles of permeate-membrane interactions, zeolite filling, and membrane swelling. *Industrial & Engineering Chemistry Research*, *44*, 7481–7489.

Nunes, S. P., & Peinemann, K. V. (2001). *Membrane technology in the chemical industry*. New York: Wiley-VCH.

Park, N. G., Schlichthörl, G., van de Lagemaat, J., Cheong, H. M., Mascarenhas, A., & Frank, A. J. (1999). Dye-sensitized TiO_2 solar cells: structural and photoelectrochemical characterization of nanocrystalline electrodes formed from the hydrolysis of $TiCl_4$. *The Journal of Physical Chemistry B*, *103*, 3308–3314.

Patil, M. B., Veerapur, R. S., Patil, S. A., Madhusoodana, C. D., & Aminabhavi, T. M. (2007). Preparation and characterization of filled matrix membranes of sodium alginate incorporated with aluminum-containing mesoporous silica for pervaporation dehydration of alcohols. *Separation and Purification Technology*, *54*, 34–43.

Patil, M. B, & Aminabhavi, T. M. (2008). Pervaporation separation of toluene/alcohol mixtures using silicalite zeolite embedded chitosan mixed matrix membranes. *Separation and Purification Technology*, *62*, 128–136.

Poschmann, M., & Ulrich, J. (1996). Fractional suspension crystallization with additional purification steps. *Journal of Crystal Growth*, *167*, 248–252.

Ragaini, V., Guaita, C., & Pirola, C. (2007). The beneficial influence of ultrasound in the polymerization of ε-caprolactam to polyamide-6 (Nylon 6). Part I. Primary experimental results. *Ultrasonics Sonochemistry*, *14*, 680–688.

Razavi, S., Sabetghadam, A., & Mohammadi, T. (2011). Dehydration of isopropanol by PVA–APTEOS/TEOS nanocomposite membranes. *Chemical Engineering Research and Design*, *89*, 148–155.

Reddy, K. M., Sairam, M., Babu, V. R., Subha, M. C. S., Rao, K. C., & Aminabhavi, T. M. (2007). Sodium alginate-TiO_2 mixed matrix membranes for pervaporation dehydration of tetrahydrofuran and isopropanol. *Designed Monomers and Polymers*, *10*, 297–309.

Ruan, D., Zhang, L. N., Mao, Y., & Zeng, M. (2004). Microporous membranes prepared from cellulose in NaOH/thiourea aqueous solution. *Journal of Membrane Science*, *241*, 265–274.

Sairam, M., Naidu, B. V. K., Nataraj, S. K., Sreedhar, B., & Aminabhavi, T. M. (2006). Poly(vinyl alcohol)-iron oxide nanocomposite membranes for pervaporation dehydration of isopropanol, 1,4-dioxane and tetrahydrofuran. *Journal of Membrane Science*, *283*, 65–73.

Sairam, M., Patil, M. B., Veerapur, R. S., Patil, S. A., & Aminabhavi, T. M. (2006). Novel dense poly(vinyl alcohol)–TiO_2 mixed matrix membranes for pervaporation separation of water–isopropanol mixtures at 30 °C. *Journal of Membrane Science*, *281*, 95–102.

Shirazi, Y., Tofighy, M. A., & Mohammadi, T. (2011). Synthesis and characterization of carbon nanotubes/poly vinyl alcohol nanocomposite membranes for dehydration of isopropanol. *Journal of Membrane Science*, *378*, 551–561.

Singha, N. R., Parya, T. K., & Ray, S. K. (2009). Dehydration of 1, 4-dioxane by pervaporation using filled and crosslinked polyvinyl alcohol membrane. *Journal of Membrane Science*, *340*, 35–44.

Veerapur, R. S., Patil, M. B., Gudasi, K. B., & Aminabhavi, T. M. (2008). Poly(vinyl alcohol)-zeolite T mixed matrix composite membranes for pervaporation separation of water + 1,4-dioxane mixtures. *Separation and Purification Technology*, *58*, 377–385.

Veerapur, R. S., Gudasi, K. B., & Aminabhavi, T. M. (2008). Sodium alginate–magnesium aluminum silicate mixed matrix membranes for pervaporation separation of water–isopropanol mixtures. *Separation and Purification Technology*, *59*, 221–230.

Wang, L., Li, J., Lin, Y., & Chen, C. (2009). Crosslinked poly(vinyl alcohol) membranes for separation of dimethyl carbonate/methanol mixtures by pervaporation. *Chemical Engineering Journal*, *146*, 71–78.

Wijmans, J. G. (2003). Letter to the Editor. *Journal of Membrane Science*, *220*, 1–3.

Yang, G., Zhang, L., Peng, T., & Zhong, W. (2000). Effects of Ca^{2+} bridge cross-linking on structure and pervaporation of cellulose/alginate blend membranes. *Journal of Membrane Science*, *175*, 53–60.

Yang, Y., Zhang, H., Wang, P., Zheng, Q., & Li, J. (2007). The influence of nano-sized TiO_2 fillers on the morphologies and properties of PSF UF membrane. *Journal of Membrane Science*, *288*, 231–238.

Zhang, L., Yu, P., & Luo, Y. (2006). Separation of caprolactam-water system by pervaporation through crosslinked PVA membranes. *Separation and Purification Technology*, *52*, 77–83.

Zhang, L., Yu, P., & Luo, Y. (2007a). Dehydration of caprolactam–water mixtures through cross-linked PVA composite pervaporation membranes. *Journal of Membrane Science*, *306*, 93–102.

Zhang, L., Yu, P., & Luo, Y. (2007b). Comparative behavior of PVA/PAN and PVA/PES composite pervaporation membranes in the pervaporative dehydration of caprolactam. *Journal of Applied Polymer Science*, *103*, 4005–4011.

Zhang, Q. G., Liu, Q. L., Shi, F. F., & Xiong, Y. (2008). Structure and permeation of organic-inorganic hybrid membranes composed of poly(vinyl alcohol) and polysilisesquioxane. *Journal of Materials Chemistry*, *18*, 4646–4653.

Zhu, T., Luo, Y., Lin, Y., Li, Q., & Yu, P. (2010). Study of pervaporation for dehydration of caprolactam through blend NaAlg–poly(vinyl pyrrolidone) membranes on PAN supports. *Separation and Purification Technology*, *74*, 242–252.